Steel and Composite Structures, *Vol. 16, No. 1 (2014) 1-21*
DOI: http://dx.doi.org/10.12989/scs.2014.16.1.001

Experimental and analytical investigations on seismic behavior of ductile steel knee braced frames

Seyed Mehdi Zahrai [1a] and Meysam Jalali [*2]

[1] *Center of Excellence for Engineering and Management of Civil Infrastructures, School of Civil Engineering, the University of Tehran, Tehran, Iran*
[2] *Department of Civil Engineering, Faculty of Engineering, University of Damghan, Damghan, Iran*

(*Received November 11, 2011, Revised August 30, 2013, Accepted September 16, 2013*)

Abstract. Knee Braced Frame (KBF) is a special form of ductile eccentrically braced frame having a diagonal brace connected to a knee element, as a hysteretic damper, instead of beam-column joint. This paper first presents an experimental investigation on cyclic performance of two knee braced single span one-story frame specimens. The general test arrangement, specimen details, and most relevant results (failure modes and hysteretic curves) are explained. Some indexes to assess the seismic performance of KBFs, including ductility**;** response reduction factor and energy dissipation capabilities are also subsequently discussed. Experimental results indicate that the maximum equivalent damping ratios achieved by test frames are 21.8 and 23% for the specimens, prior to failure. Finally, a simplified analytical model is derived to predict the bilinear behavior of the KBFs. Acceptable conformity between analytical and experimental results proves the accuracy of the proposed model.

Keywords: knee braced frames; cyclic behavior; ductility; equivalent damping ratio; response reduction factor; simplified model

1. Introduction

Structures designed to resist moderate and frequently occurring earthquakes must have sufficient stiffness and strength to control deflection and to prevent any possible damage. However, it is inappropriate to design a structure to remain in the elastic region under severe earthquakes, because of the economic constraints. The inherent damping of yielding structural elements can be advantageously utilized to lower the strength requirement, leading to a more economical design. This yielding capability usually provides the ductility or toughness of the structure against the sudden brittle type of structural failure. Since stiffness and ductility are generally two opposing properties (AISC 2005), it is desirable to devise a structural system that combines these properties in the most effective manner without excessive increase in the cost. In steel structural systems, Moment Resisting (MRF) and Concentrically Braced Frames (CBF) have been widely used to resist earthquake loads. The MRF possesses good ductility through flexural yielding of beam elements, but it has limited lateral stiffness to control deflections. Further concern on the structural

∗Corresponding author, Assistant Professor, E-mail: mjalali@du.ac.ir
[a] Professor, E-mail: mzahrai@ut.ac.ir

http://www.techno-press.org/?journal=scs&subpage=8 ISSN: 1229-9367 (Print), 1598-6233 (Online)

performance of MRF attributes to the beam to column connection design. Higher demand is required in the connections if sufficient ductility is desired (Abdalla *et al*. 2007, Ciutina and Dubina 2006, Lehman *et al*. 2008, Pucinotti 2006, Yoo *et al*. 2008).

The CBF on the other hand is too stiff, and its ductility is limited because of buckling of the diagonal brace. In addition to the ductility concern, the design requirements, as well as the fabrication costs, for the brace members are usually high, because those members are required to exhibit effective buckling strength and adequate post-buckling performance during earthquake excitation (Lee and Bruneau 2005, Uriz *et al*. 2008). To overcome the deficiencies in MRF and CBF, Roeder and Popov (1978) have proposed the Eccentrically Braced Frame (EBF) system, where the brace is intentionally placed eccentric to the beam–column joint. Using a suitable choice of eccentricity, a sufficient amount of lateral stiffness from the brace is retained while ductility is achieved through the flexural and/or shear yielding of a segment of the beam, which is called the link, created by the eccentrically connected brace member. To achieve the required ductility, however, severe yielding of the link is expected, which at the same time may lead to serious floor damage. Further, as the link is an integral part of a main structural member, retrofitting may be difficult. As an alternative to the commonly used structural systems, a Knee-Braced-Frame (KBF) was proposed by Balendra *et al*. (1990). That was a new bracing system where the diagonal brace was anchored to a short member instead of the beam-column joint. This short member called "knee element" was designed to yield in flexure, whereby buckling of the brace was prevented. The proposed KBF system was different from the one previously proposed by Aristizabal-ochoa (1986) where the brace had been designed for tension only. In another study by Balendra *et al*. (1994), the KBF was designed in such a way that the knee yields in shear instead of flexural under strong ground motions. A 50 mm × 50 mm built-up I-section was used in a one story KBF to study the inelastic behavior. When the knee member was designed against local buckling and lateral torsional buckling, un-pinched hysteretic loops were obtained without any significant deterioration in lateral strength or stiffness. Moreover, Balendra *et al*. (1997) accomplished a pseudo-dynamic test on a two story KBF with rolled I-sections as knee members. Their test results revealed that the variation of shear stresses with the shear strain in the knee could have been approximated by a bilinear curve with a strain-hardening slope of 0.02-0.04. In KBFs, the damage is concentrated in a secondary member, which can be easily repaired at minimum cost. Floor distortions are reduced compared to the case for the EBF, to a level similar to that of the conventional MRF and CBF. Recently Hsu *et al*. (2011) have introduced an alternative KBF system, in which knee member remains in elastic rang while dissipation occurs in story beam. Hence, the concept of this KBF system is different from what produced by Balendra *et al*. (1994).

This paper reports on a test program performed on braced frames having Knee Elements as their hysteretic dampers. Two full-scale tests were conducted on steel braced frames in order to find out key issues influencing cyclic behavior of KBFs. The cyclic performance of the frames was evaluated in terms of strength, ductility and energy dissipation. In addition, lateral torsional buckling potential of knee member was inspected. All tests were of the cyclic quasi-static type for which similar displacement time histories were considered. At last, a simplified analytical model was derived to predict the stiffness of the braced frames having knee elements as their hysteretic dampers. This analytical model was evaluated and compared with experimental results.

Most specific contributions of this paper are summarized here: (1) experimental work on knee braced frame by cyclic testing of 2 full-scale frame specimens; (2) studying the capability of using knee bracing system in simple frames (as such systems have been mostly used already in moment frames); (3) application of IPE sections for the knee member (previous researchers have mostly

studied Wide flange sections (IPB) as the link beam of KBF); (4) investigation of relatively high yield stress of steel link beam on the cyclic performance (as typical steel in the market is usually with 3000-3500 kg/cm^2 as yield stress instead of 2400 kg/cm^2); and (5) using short link beam such that no lateral support is needed.

2. Experimental program

An experimental program was undertaken to establish the actual performance of the KBFs in structural laboratory of Building and Housing Research Center of Iran (BHRC). In this program, two full scale single span single-story models were fabricated and tested. The following sections describe the KBF design approach, the main features of test set-up, and the applied load protocol.

2.1 Design approach

The philosophy of design for the KBF is that in the event of a strong earthquake, the knee element should yield and dissipate energy through shear or flexural yielding before any damage can occur to other members, thereby preserving the main structural elements. The design is based on the load-carrying capacity of one side of knee element (as the knee element is divided into two parts by diagonal brace). According to this concept, for design of first KBF specimen (that is called KBF1 henceforth), it was assumed that only shorter part of knee element would experience inelastic shear deformations and the other part of knee element would remain elastic. This approach is similar with that usually considered in EBFs. The accuracy of this assumption will be evaluated later. According to this methodology, the knee element was pre-selected and the other members including columns, beam, and diagonal brace, were proportioned based on the shorter part of knee element shear strength.

Note that the knee member must be designed to satisfy several conditions simultaneously. It must have the desired shear strength, flexural strength, and link length, having met the limits for flange compactness and web compactness. The specimens were designed according to AISC (2005) Seismic provisions, similar with EBF systems. It was decided to test a shear link instead of flexural one, as these were deemed more likely to be used in practical applications (partly due to their larger rotation limits). The knee element must also resist against premature failure due to local and lateral torsional buckling.

Five full depth stiffeners were welded on the knee element web to provide its complete shear yielding behavior. The actual material characteristics of the steel specimens were determined from testing of tensile coupons taken from the knee member sections, and were tested in accordance with the ASTM (2003) Standard. Specifications of the specimens are given in Table 1.

Table 1 Specifications of the test specimens

Spec.	Web stiffeners		Knee		Brace		Beam		Column		Steel properties	
	Distance (mm)	Thickness (mm)	Length (mm)	Section	Length (mm)	Section	Length (mm)	Section	Length (mm)	Section	F_y (N/mm^2)	F_u (N/mm^2)
KBF1	100	10	800	IPE140	4300	2UNP80	3600	IPE180	3500	2IPE140	333.9	482.7
KBF2	100	10	800	IPE120	4300	2UNP100	3600	IPE180	3500	2IPE140	322.9	468.0

Based on the seismic provisions, the required shear strength of the link (Knee element), V_u, shall not exceed the design shear strength of the link φV_n, where

$$\begin{aligned} V_n &= \text{Nominal shear strength of the link, equal to the lesser of } V_p \text{ or } 2M_p e, \\ V_p &= 0.60F_y(d-2t_f)t_w \\ \varphi &= 0.90 \end{aligned} \tag{1}$$

and e, F_y, d, t_f, and t_w are the link length (link implies to knee element), specified minimum yield stress of the steel, link depth, flange, and web thickness of the link, respectively. The beam-column connections were designed to be moment resisting, generally considering the FEMA (2000) requirements for pre-qualification details.

2.2 Test set-up

Two different subassemblies in two different details were tested, each with the same beam-column components but different lateral bracing design. Usual practice would use fillet welds for the gusset plate attachment. The frame was mounted on clevises at the base of each column fastened to a foundation beam attached to the strong floor of the BHRC (Building & Housing Research Center, Iran) structural laboratory. Two reaction frames, also attached to the strong floor, were used to mount the actuators applying lateral load. Fig. 1 shows general configuration of the test frame. Note that excluding the clevis heights, the actual height of the specimen from the centerline of the beam to the centerline of the clevises was set at 3500 mm. The frame subassemblies were extensively instrumented. Instrumentation included displacement transducers for global frame and knee-brace out-of-plane displacements, and strain gauges (KFG1011) to allow subsequent determination of frame stresses and forces. Strain gauges (YEFLA5, 2) were also included in the knee element to show its inelastic behavior.

For safety purposes and to simulate the floor diaphragm, the beam was globally braced against out-of-plane instability at six points on the loading beam by using the cables available in the BHRC structural laboratory, as observed in Fig. 1; however, no lateral bracing was provided to the knee element itself.

(a)

Fig. 1 General configuration of the test frame: (a) Photo of specimen and set-up; (b) schematic view of test set-up and instrumentations

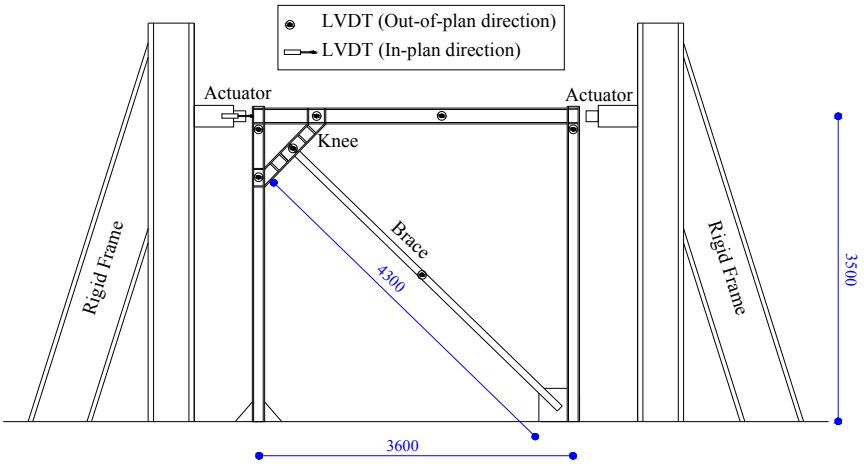

(b)

Fig. 1 Continued

2.3 Loading protocols

The quasi-static loading protocol used here was developed based on the guidelines presented in AISC (2005) Seismic provisions. The story drift sequence was applied by two single-action 1000 kN actuators running in alternation. In order to assess a reasonable value of yielding displacement, force-control load history was applied to the test frame before appearance of yielding on the knee member. Verification of the yield force was carried out by checking the values for the principal strains from the rosettes on the web of the link and general behavior of the entire test frame. Beyond yield displacement, the subsequent cycles were applied in displacement-control using the horizontal displacement recorded at the beam level. Fig. 2 shows the general loading protocol.

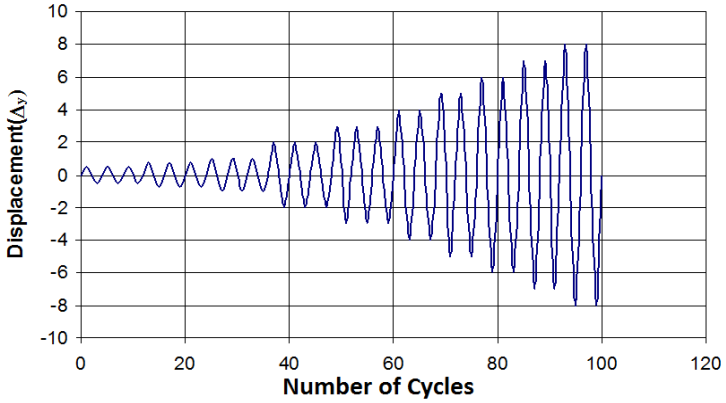

Fig. 2 Applied load protocol according to AISC recommendations

Fig. 3 Yielding of the second panel at 10th cycle of lateral loading

(a) Local yielding of diagonal brace at 18.9 mm lateral displacement

(b) Overall buckling of diagonal brace at 22.3 mm lateral displacement

Fig. 4 Interruption of KBF1 test due to undesirable buckling of diagonal brace

3. Experimental results

Expanded descriptions of Specimens' hysteresis behavior and failure modes are presented here.

3.1 Specimen KBF1

For the sake of convenience, Knee element is nominally categorized to panels between stiffeners, the upper-most one called "first panel" and so on for other panels. At the lateral force of 80 kN imposed to the top of the specimen, the principal strains on the web of the second panel of knee element, exceeded from steel yield level. In spite of this local yielding, overall behavior of test frame remained linear. Eventually, top lateral force of 120 kN, corresponding to 6.3 mm lateral displacement, was estimated as the yielding force of the test frame. Fig. 3 shows the flaked whitewash on the second panel at the 10th cycle of lateral loading corresponding to top lateral force of 120 kN.

At the lateral displacement of 18.1 mm, almost all panels experienced plastic deformations. The undesirable failure mode of the KBF1 specimen was the overall buckling of the diagonal brace at 22.3 mm lateral displacement. The fracture was assessed as initiated by appearance of local

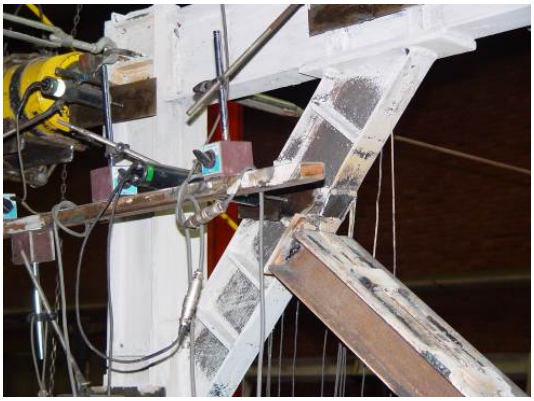

Fig. 5 Termination of KBF1 test by fracture of knee-diagonal brace weld at KBF1 test specimen

yielding on the batten plate of diagonal brace. Fig. 4(a) shows the initiation and overall buckling of diagonal brace. Considerable values of out-of-plane deformations took place on diagonal brace (Fig. 4(b)).

The most important factor that was likely contributed to this failure refers to the KBF design assumption. As mentioned earlier, it was assumed that only one side of the knee element would encounter plastic strains, whereas the experimentally observed regions of yielding comprise both sides of the knee member. As seen in Fig. 3, in the primary cycles of displacements, yielding appeared on one side of knee element, then yielding at the other side of knee member occurred due to increase of lateral displacement. This indicates that, due to expansion of yielding areas on the knee element, axial force demand on the diagonal brace was increased and led to its overall buckling. As a result, this method of design was modified for KBF2 test specimen to improve its behavior.

After the interruption of test at fist part, the diagonal brace was repaired and strengthened by two similar back-to-back channel sections. After that, the test was continued up to failure of knee-

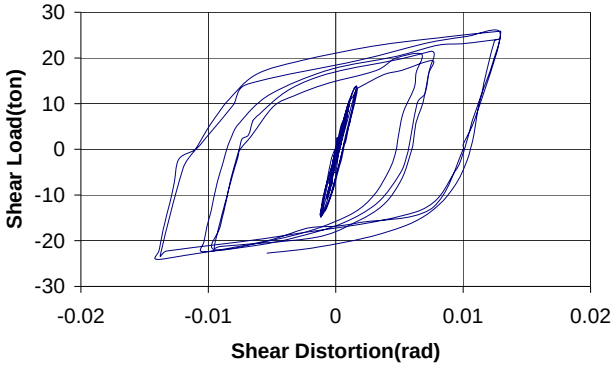

(a) Hysteretic behavior of knee element

Fig. 6 Hysteretic behavior of KBF1 test specimen

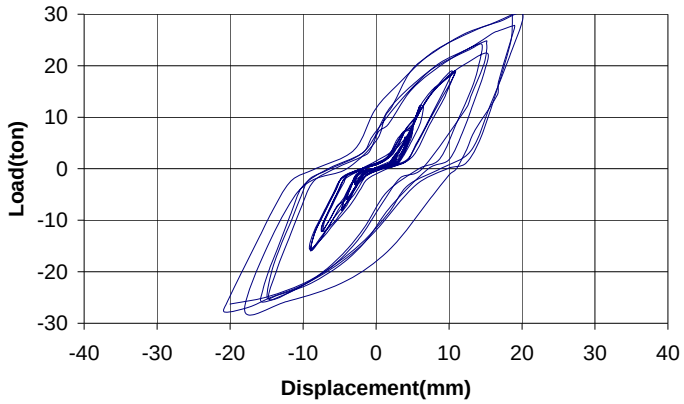

(b) Overall hysteretic behavior

Fig. 6 Continued

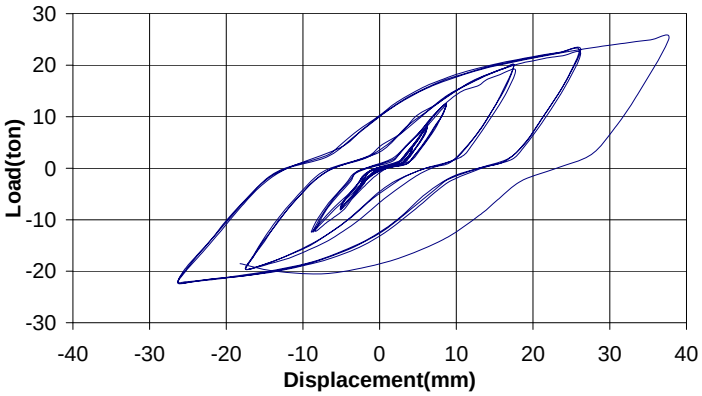

Fig. 7 Overall hysteretic behavior of entire KBF2 specimen

knee-diagonal brace connection weld at 24.3 mm lateral displacement. Actually, at second part of this test, only two cycles of loading were sustained by test frame. However, this failure was predictable since the weld was not supposed to experience the forces delivered by new section. Fig. 5 shows the failure of test frame after the strengthening.

Fig. 6(a) shows the corresponding link shear force versus link rotation hysteresis curves. The maximum link shear force and shear distortion were 259 kN and 0.014 rad, respectively, this rotation is an inappropriate seismic characteristic and occurred due to overall buckling of diagonal brace as described earlier. Typical hysteresis curves obtained from KBF1 test are presented in Fig. 6(b). As shown in this figure, a little slip has occurred at column supports throughout the test, which is eliminated for estimation of yielding displacement. Taking into consideration projections of the elastic and inelastic slopes of hysteresis curve of test frame on Fig. 8, the modified yield lateral force was approximately 152 kN corresponding to lateral displacement of 5.7 mm. The maximum base shear and displacement were 300 kN and 20.1 mm, respectively. Therefore, the ductility of first prototype is approximately 3.5.

3.2 Specimen KBF2

Highlights of the test results are provided here. The frame subassembly overall demonstrated very good behavior through the entire sequence of cycles and before failure of test frame (Fig. 7). The frame peak forces are extremely consistent in opposing directions as well as from cycle to cycle, implying similarly consistent behavior for reversal loading.

Evidence of yielding became apparent on the second panel at 123 kN lateral force corresponding to 8.7 mm top lateral displacement as shown in Fig. 8(a). Weaker signs of yielding was also appeared on third and fifth panels, these values were assessed as yielding value of KBF2 (the force that caused yielding of knee element). Tenth cycle of loading (first cycle of $2\Delta_y$ displacement) corresponding to lateral displacement of 17.5 mm was the initiation of yielding on the other panels. Fig. 8(b) reveals that almost all panels experienced plastic deformations at eleventh cycle. At the 14th cycle of loading, equal to 26.1 mm lateral displacement, some evidence of yielding appeared on the bottom flange of upper part of knee element. Third cycle of $3\Delta_y$ lateral displacement (15^{th} cycle) was corresponding to plastic deformations and local buckling of knee flange in vicinity of knee-brace connection. Finally, at the top lateral displacement of $4\Delta_y$ the test was terminated due to tearing on the web of knee element at the face of knee-brace connection as shown in Fig 8(c).

(a) Yielding of the second panel at 7th cycle of loading

(b) Yielding of the 5th and 7th panels at 11th cycle of loading

(c) Tearing on the web of knee element at third panel

Fig. 8 Yielding sequence of knee element at KBF2 test specimen

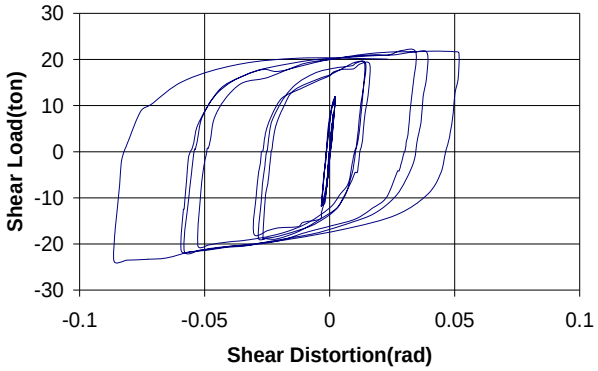

Fig. 9 Hysteretic behavior of knee element – KBF2 specimen

Fig. 9 shows the corresponding link shear force versus link shear distortion hysteresis. The maximum link shear force and shear distortion were 235 kN and 0.086 *rad*, respectively. Note that the current shear distortion limit for shear links in EBFs is 0.08 rad. There was no evidence of crack initiation in welds or any sign of failure in other members. Slip displacement is omitted similar with KBF1. Taking projections of the elastic and inelastic slopes of Fig. 7 into consideration, the modified yield lateral force was approximately 136 kN corresponding to lateral displacement of 7 mm. The maximum base shear and displacement were 251 kN and 37.7 mm, respectively. Therefore, the ductility of KBF2 was obtained about 5.4. Note that different range of horizontal axis was used in Figs. 6(a) and 9.

Bolted supports, connecting both columns to strong floor of structural laboratory caused a little slip at column supports throughout the tests. This slip led to a slight pinching in overall hysteretic behavior of specimens, as observed in Figs. 6(b) and (7). However, this pinching is not observed in hysteretic behavior of knee element in Figs. 6(a) and 9, as it was obtained using shear load versus shear distortion (both for just the knee member), which is not affected by little slip of the frame at its base.

3.3 Lateral torsional buckling potential

Out-of-plane movements at the knee-brace connection, implying LTB (Lateral Torsional Buckling) of knee element, were reported very small as shown in Fig. 10. Therefore**,** no lateral bracing seems to be essentially required for knee-brace connection. Because of overall buckling of diagonal brace in KBF1 test specimen, larger out-of-plane movements at KBF1 were found in contrast with KBF2 as compared in Figs. 10(a) and (b).

4. Determination of response modification factor

In force-based seismic design procedures, response modification factor (or reduction factor), R (or R_w), also referred to by other terms including, reduction factor, is the ratio of the strength required to maintain the structure elastic to the inelastic design strength of the structure. The reduction factor, R, therefore accounts for the inherent ductility and over-strength of a structure and

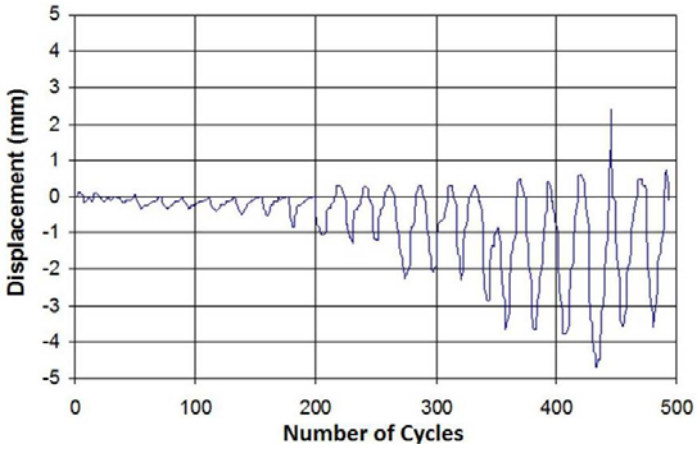

(a) KBF1 test specimen

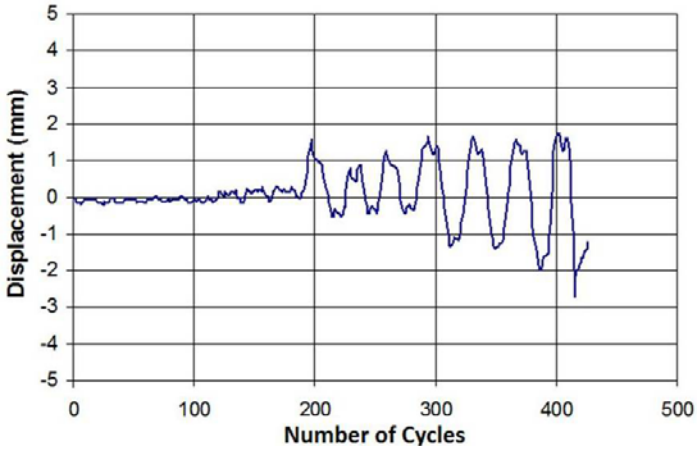

(b) KBF2 test specimen

Fig. 10 Out-of-plane movement at Knee-Brace connection

the difference in the level of stresses considered in its design. It is generally expressed in the following form taking into account the above three components.

$$R = R_{\mu} . \Omega . Y \tag{2}$$

where, R_{μ} is the ductility-dependent component also known as the ductility reduction factor. It indicates the capacity of the frame for energy absorption. Ω is the so-called over-strength factor and Y is the allowable stress reduction factor. With reference to Fig. 11, in which the actual force–displacement response curve is idealized by a bilinear elastic–perfectly plastic response curve, the reduction factor parameters may be defined as

$$R_{\mu} = C_e . C_y , \quad \Omega = C_y / C_s , \quad Y = C_s / C_w \tag{3}$$

Moreover, the reduction factor, R, is redefined as

$$R(R_w) = (C_e / C_y) \cdot (C_y / C_s) \cdot (C_s / C_w) = C_e / C_w \tag{4}$$

where, C_e, C_y, C_s and C_w correspond to the equivalent base shear force required to represent the load effect for elastic analysis purposes, the idealized yield strength, the first significant yield strength and the allowable stress design strength (as defined by conventional design codes), respectively.

When the used design method is based on ultimate strength, the allowable stress reduction factor, Y, is equal to unity and the reduction factor is reduced to

$$R = R_\mu \cdot \Omega = C_e / C_s \tag{5}$$

The structure ductility, μ, is defined in terms of maximum structural drift (Δ_{max}) and the displacement corresponding to the idealized yield strength (Δ_y) as

$$\mu = \Delta_{\max} / \Delta_y \tag{6}$$

Ductility reduction factor R_μ is a function of both characteristics of the structure including ductility, damping and fundamental period of vibration (T), and characteristics of earthquake ground motion. Many investigators have discussed the two main components of R factor presented in Eq. (5), in particular, the ductility dependent component, R_μ, has received considerable attention. One of these discussions can be seen in Miranda and Bertero (1994) work in which they showed the T-dependence of R_μ. They also demonstrated the influence of underlying soil type on the values of ductility reduction factor, R_μ as bellow

$$R_\mu = \frac{\mu - 1}{\Phi} + 1 \ \geq \ 1 \tag{7}$$

Φ is a function of T and μ. This parameter is different for rocky, sedimentary or alluvial bases.

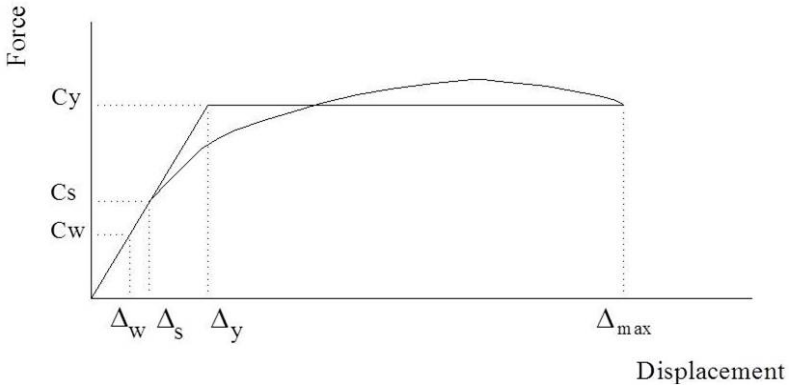

Fig. 11 Parameters used in calculation of ductility, over-strength factor and allowable reduction factor

Table 2 Reduction factors of test specimens

Spec.	H (mm)	T (s)	Δ_{max} (mm)	Δ_y (mm)	μ	R_μ	C_y (kN)	C_s (kN)	Ω	Y	R
KBF1	3500	0.128	18.03	9.89	1.82	1.42	299.6	122	2.46	1.42	4.96
KBF2	3500	0.128	35.66	12.95	2.75	1.84	251.3	118	2.13	1.43	5.63

Reduction factor of test frames is calculated in accordance with Miranda and Bertero (1994) relationship.

Since there was no interaction between the test frames and bases, it is not irrational to use rocky equation in order to calculate the Φ parameter

$$\Phi = 1 + \frac{T}{10T - \mu T} - \frac{1}{2T}\exp\left(-\frac{3}{2}\left(\ln T - \frac{3}{5} \right)^2 \right) \tag{8}$$

Table 2 demonstrates the reduction factor of each test specimen considered in this paper. Note that Y factor has been calculated based on Zahrai (2006). As observed from Table 2, the ductility values should be increased in order to improve acquired reduction factors. This would take place due to change of those characteristics of models dealing with this parameter.

5. Energy dissipation

It is generally accepted that energy dissipated in cyclic straining of metals is rate-independent (Chan and Albermani 2008). In order to capture the energy dissipation characteristics of each specimen configuration at a given displacement amplitude, an equivalent viscous damping ratio, ξ_{eq}, representative of the hysteretic damping in the frame, was computed from the global hysteretic behavior of each specimen configuration. The ratio of dissipated energy to conserved energy is recommended to estimate the damping ratio of a structure due to its passive energy dissipation devices (Chopra 2007)

$$\xi_{eq} = \frac{A_h}{4\pi A_e} \tag{9}$$

where A_h is area enclosed by one complete cycle of the force-displacement response for an energy dissipation device at a desirable displacement amplitude, and A_e is elastic strain energy conserved per cycle, corresponding to effective stiffness (k_{eff}) (Chopra 2007)

$$A_e = \frac{k_{eff}\Delta_{ave}^2}{2}, \quad k_{eff} = \frac{\left|F^-\right| + \left|F^+\right|}{\left|\Delta^-\right| + \left|\Delta^+\right|} \tag{10}$$

In which K_{eff} and Δ_{ave} are effective stiffness and average displacement of an energy dissipation unit during a cycle of prototype testing, equal to $(|\Delta^+| + |\Delta^-|)/2$, where displacements Δ^- and Δ^+ are negative and Positive displacement amplitude during a cycle of prototype testing. Forces F^- and F^+

Table 3 Parameters used in calculation of equivalent viscous damping ratio on last cycles

Spec.	A_h (kN.mm)	V_{max} (kN)	V_{min} (kN)	V_m (kN)	Δ_{max} (mm)	Δ_{min} (mm)	Δ_m (mm)	ξ_{eq} (%)
KBF1	6960	278.46	270	274.23	18.99	18.01	18.50	21.80
KBF2	8630	231.63	223.28	227.45	26.20	26.30	26.25	23.00

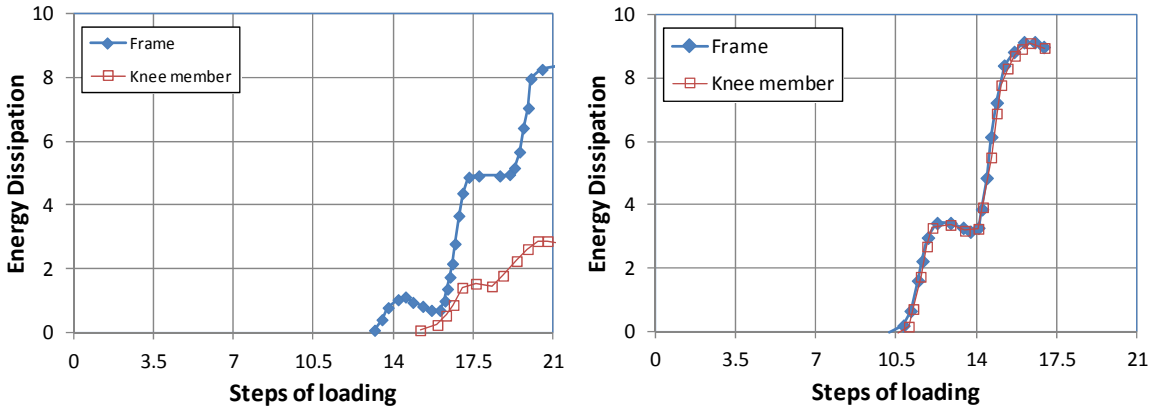

(a) KBF1 test specimen (b) KBF2 test specimen

Fig. 12 Comparative energy dissipation

are Negative and positive forces during a single cycle of prototype testing at a displacement amplitude of Δ^- and Δ^+. Table 3 presents equivalent viscous damping ratio of the test specimens for the last cycle, in details. In the same way, this ratio is calculated for other cycles of loading (Zahrai 2006). Finally, the mean value of equivalent viscous damping ratios for KBF1 and KBF2 were obtained 16.8 and 18.6 percent respectively, whereas the maximum values were 21.8 and 23 percent corresponding to last cycle.

Comparative energy dissipation of entire test frames and knee members (hysteretic dampers) are available at Fig. 12. At these figures, horizontal axis depicts cycle of loading and vertical axis corresponds to normalized dissipated energy. For the sake of normalization, dissipated energy values are divided to product of frame shear yield force and frame yield displacement. At KBF1 due to buckling and hence occurring of local yielding on diagonal brace, maximum capacity of knee member has not been mobilized for dissipation of imposed energy. As observed in Fig. 12 (a), the differences between two curves are dominantly caused by energy absorption of diagonal brace. As a result, use of two components for energy dissipation simultaneously, caused improper seismic characteristics of system as observed in KBF1. Unlike KBF1, at the KBF2 almost all of energy dissipation has taken place on the knee member and the maximum normalized energy by the frame and also knee member is about 9 in Fig. 12 (b). Whereas for KBF1 test specimen, this value is equal to 8.3 for entire test frame and 2.8 for knee member.

6. Simplified analytical model

A simplified analytical model is presented here to predict bilinear force-displacement

relationship of one-story one-bay knee braced frame. In low level of lateral loads, braced frame remains mainly elastic, and the knee element is not activated. In this case, the lateral stiffness of the whole frame is provided mainly by the elastic lateral stiffness of the braces and knee member. However, as lateral loads increase, the knee element gradually enters the plastic range, resulting in reduction of the frame lateral stiffness and increase of ductility. Consequently, the response of a braced frame with knee member (Fig. 13(a)) can be divided into elastic and plastic parts:

6.1 Elastic lateral stiffness of frame

The elastic lateral stiffness of KBF, which is called K_{ebf}, (*ebf* is standing on elastic braced frame) can be evaluated as follows (see appendix for details)

$$k_{ebf} = \frac{\cos^2(\phi)}{\frac{\frac{L_{dke}^3 L_{uke}^3}{3EI_k L_k^3} + \frac{L_{dke}^2 L_{uke}^2}{3EI_k L_k}}{2} + \frac{L_d}{EA_d}} \tag{11}$$

where ϕ indicates the diagonal brace-beam angle; E, A_d, and L_d are Young modulus, cross sectional area and length of diagonal braces, respectively. The parameters L_{dke}, L_{uke}, I_k and L_k are length of lower part, length of upper part, moment of inertia and entire length of knee member. Due to insignificant lateral stiffness of moment frame in comparison with total lateral stiffness, it was neglected in evaluating K_{ebf}.

6.2 Plastic lateral stiffness of frame and analytical model development

Consider a moment frame braced by knee bracing system, as shown in Fig. 13(a). Assuming that the braces can provide an extremely stiff region, the frame may be modeled as shown in Fig. 13(b).

The model consists of three parallel springs due to their identical deflections: an elastic spring designated by k_{mf} and two elasto-plastic springs, designated by k_{uke} and k_{dke}. The parameters k_{mf}, k_{uke} and k_{dke} indicate the elastic stiffness of the moment frame, plastic stiffness of lower part and that of upper part of knee element, respectively. Since the moment frame is to remain elastic during lateral loading, the stiffness k_{mf} can readily be derived by the elastic analysis of the frame, as follows (see appendix for details)

$$k_{mf} = \frac{12EI_c}{L_c^3}\left[\frac{I_c / L_c + 6I_b / L_b}{2I_c / L_c + 3I_b / L_b}\right] \tag{12}$$

In which E is Young's modulus; I_b and I_c are, respectively, beam and column moment of inertia; L_b and L_c are length of beam and column, respectively. For a shear panel exposed to shear deformations, lateral stiffness through web direction can be evaluated by following expressions (Krawinkler 1978)

$$\begin{aligned} k &= (0.95 d_{sp} t_{sp} G)/L_{sp} && for \quad 0 \le \gamma \le \gamma_y \\ k &= (1.095 b_{spf} t_{spf}^2 G / L_{sp})/L_{sp} && for \quad \gamma_y \le \gamma \le 4\gamma_y \end{aligned} \tag{13}$$

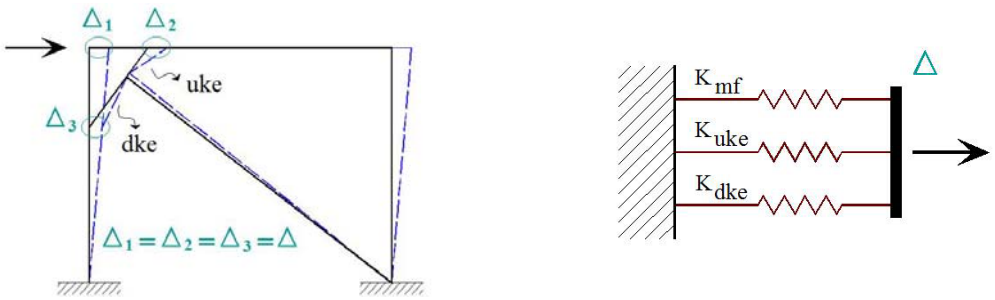

(a) (b)

Fig. 13 (a) Moment frame braced by knee bracing system; (b) stiffness model for the frame

In which G, γ and γ_y are the shear modulus, the shear panel distortion, and the shear distortion at general yielding, respectively. d_{sp}, t_{sp}, b_{spf} and t_{spf} are web depth, web thickness, flange width and flange thickness of the shear panel, respectively. L_{sp} is the net length of the shear panel. If constitutive behavior of steel material is assumed as a bilinear curve, for shear distortion greater than $4\gamma_y$, a constant strain hardening stiffness describes the shear panel (knee element) performance. Since the shear distortion of the upper part of knee element is usually much more than $4\gamma_y$ (γ_y is 0.0017 for F_y = 240 N/mm^2), it is not irrational to take k_{uke} as $(0.95 d_{sp} t_{sp} G_s)/L_{sp}$, where G_s is equal to tangent modulus of steel material. Based on experimental assessment, lower part of knee element indicated more limited signs of yielding with respect to upper part (for proposed geometry in this paper), thus k_{dke} can be estimated by $(1.095 b_{spf} t^2_{spf} G/L_{sp})/L_{sp}$. In these equations, the direction of stiffness is perpendicular to element axis and it can be proven to be accurate for desirable directions (see Fig. 13(a)).

$_{sp}$ index is referred to shear panel and for knee element it is replaced by k_e index. Finally inelastic stiffness of knee braced frame, k_{iebf}, can be expressed as following

$$k_{iebf} = k_{mf} + k_{uke} + k_{dke} \tag{14}$$

$$k_{iebf} = \frac{12 E I_c}{L_c^3}\left[\frac{I_c / L_c + 6 I_b / L_b}{2 I_c / L_c + 3 I_b / L_b}\right] + 0.95 d_{ke} t_{ke} G_s / L_{ke} + (1.095 b_{kef} t_{kef}^2 G / L_{ke}) / L_{ke} \tag{15}$$

It should be noted that in the above equations the effects of the shear deformation of the beam panel zones are neglected. Moreover, Δ_2 and Δ_3 in Fig. 13(a) are not equal, but for simplicity they are assumed equal. It should be noteworthy that in case of using hinged frames, k_{mf} should be ignored in Eqs. (14) and (15).

6.3 Validation of simplified analytical model

In order to verify proposed analytical model, experimental findings of elastic and inelastic parts of load-deflection response in KBF1 and KBF2 are compared by the analytical predictions in Table 4. In this table, experimental values were obtained by ignoring the initial slips in Figs. 6(b)

Table 4 Comparison of analytical and experimental results

	Specimen	Analytical (kN/mm)	Experimental (kN/mm)	Analytical/ Experimental
Elastic stiffness	KBF1	34	28	1.21
	KBF2	29	19	1.52
Inelastic Stiffness	KBF1	14	11	1.23
	KBF2	11	8	1.39

and 7. As observed, the simplified analytical model proposed for one-bay one-story KBF, predicted the lateral stiffness of KBF1 and KBF2 specimens between 21 and 52% more than experimentally measured values. The simplified analytical model can be extended to multi-story frames being able to predict capacity curve of a multi-story KBF although further research in this regard is required.

7. Conclusions

An experimental study was conducted in which the response of knee braced frames to cyclic loading was investigated. The objective of these tests was to examine performance of such systems under idealized seismic loading conditions. The specimen responses were assessed in terms of failure mode, reduction factor, energy dissipation and general hysteretic behavior. In addition, an analytical model was derived to predict the bilinear behavior of the KBF. A complete knowledge of all of these parameters was necessary for appropriate seismic assessment based on the capacity design approach, as well as for the validation of analytical models. The evaluation of the results obtained in this study leads to the following conclusions:

First test specimen exhibited undesirable hysteretic behavior due to buckling of diagonal brace, whereas after modification of design approach, the second one presented stable hysteretic behavior up to failure. It is recommended that different yielding sequences be considered in seismic analysis of KBFs.

The limited out-of-plane movements at knee-brace joint revealed a proper safety margin against lateral torsional buckling.

The maximum reduction factor and equivalent damping ratio of test specimens were 5.63 and 23% respectively, that were not relatively considerable values and thus it is concluded that the geometry of frame significantly affects on seismic performance of such systems.

Simultaneous use of two components in series for energy dissipation, the diagonal brace and knee member, resulted improper seismic characteristics of system as observed in KBF1 test specimen.

Acceptable agreement between analytical and experimental results proved the accuracy of the proposed simplified model derived to predict the bilinear behavior of the KBFs.

Acknowledgments

The authors wish to acknowledge the support provided by college of engineering at the

university of Tehran (research project 8108020/1/07) and the Building and Housing Research Center (BHRC) of Iran (Project no. 1-4560). However, the findings obtained in this research are those of the authors and not necessarily those of the sponsors.

References

AISC (2005), *Seismic Provisions for Steel Buildings*, AISC/ANSI Standard 341-05, American Institute of Steel Construction, Chicago, IL, USA.

Abdalla, K.M., Abu-Farsakh, G.A.R. and Barakat, S.A. (2007), "Experimental investigation of force-distribution in high-strength bolts in extended end-plate connections", *Steel. Compos. Struct., Int. J.*, **7**(2), 87-103.

Aristizabal-ochoa, J.D. (1986), "Disposable knee bracing: improvement in seismic design of steel frames", *J. Struct. Eng. ASCE*, **112**(7), 1544-1552.

ASTM (2003), *Standard Test Methods and Definitions for Mechanical Testing of Steel Products*, ASTM International, A370-03a, American Society for Testing and Materials.

Balendra, T., Lim, E.L. and Lee, S.L. (1994), "Ductile knee braced frames with shear yielding knee for seismic resistant structures", *Eng. Struct.*, **16**(4), 263-269.

Balendra, T., Lim, E.L. and Liaw, C.Y. (1997), "Large-scale seismic testing of knee-braced-frame", *J. Struct. Eng. ASCE*, **123**(1), 11-19.

Balendra, T., Sam, M.T. and Liaw, C.Y. (1990), "Diagonal brace with ductile knee anchor for aseismic steel frame", *Earthq. Eng. Struct. Dyn.*, **19**(6), 847-858.

Chan, R.W.K. and Albermani, F. (2008), "Experimental study of steel slit damper for passive energy dissipation", *Eng. Struct.*, **30**(4), 1058-1066.

Chopra, A.K. (2007), *Dynamics of Structures: Theory and Applications to Earthquake Engineering*, Prentice Hall, Englewood Cliffs, NJ, USA.

Ciutina, A.L. and Dubina, D. (2006), "Seismic behaviour of steel beam-to-column joints with column web stiffening", *Steel. Compos. Struct., Int. J.*, **6**(6), 493-512.

FEMA (2000), *NEHRP Recommended Seismic Design Criteria for New Steel Moment-Frame Building*, FEMA Report 350, Washington, D.C., Federal Emergency Management Agency.

Hsu, H.L., Juang, J.L. and Chou, C.H. (2011), "Experimental evaluation on the seismic performance of steel knee braced frame structures with energy dissipation mechanism", *Steel. Compos. Struct., Int. J.*, **11**(1), 77-91.

Krawinkler, H. (1978), "Shear in beam-column joints in seismic design of steel frames", *Eng. J., AISC*, **3**(15), 82-91.

Lee, K. and Bruneau, M. (2005), "Energy dissipation demand of compression members in concentrically braced frames", *Steel. Compos. Struct., Int. J.*, **5**(5), 345-358.

Lehman, D.E., Roeder, C.W., Herman, D., Johnson, S. and Kotulka, B. (2008), "Improved seismic performance of gusset plate connections", *J. Struct. Eng. ASCE*, **134**(6), 890-901.

Miranda, E. and Bertero, V.V. (1994), "Evaluation of strength reduction factors for earthquake-resistant design", *Earthq. Spectra*, **10**(2), 357-379.

Pucinotti, R. (2006), "Cyclic mechanical model of semirigid top and seat and double web angle connections", *Steel. Compos. Struct., Int. J.*, **6**(2), 139-157.

Roeder, C.W. and Popov, E.P. (1978), "Eccentrically braced steel frames for earthquakes", *J. Struct. Div., ASCE*, **104**(ST3), 391-412.

Uriz, P., Filippou, F.C. and Mahin, S.A. (2008), "Model for cyclic inelastic buckling of steel braces", *J. Struct. Eng. ASCE*, **134**(4), 619-628.

Yoo, J.H., Lehman, D.E. and Roeder, C.W. (2008), "Influence of connection design parameters on the seismic performance of braced frames", *J. Constr. Steel Res.*, **64**(6), 607-623.

Zahrai, S.M. (2006), *Behavior of Shear Link in Typical Steel Frames*, BHRC Press, Building and Housing Research Center of Iran, Tehran, Iran.

Zahrai, S.M. and Bruneau, M. (1999), "Cyclic testing of ductile end-diaphragms for slab-on-girder steel bridges", *J. Struct. Eng. ASCE*, **125**(9), 987-996.

CC

Appendix

Calculation of elastic lateral stiffness of moment frame (Eq. (12))

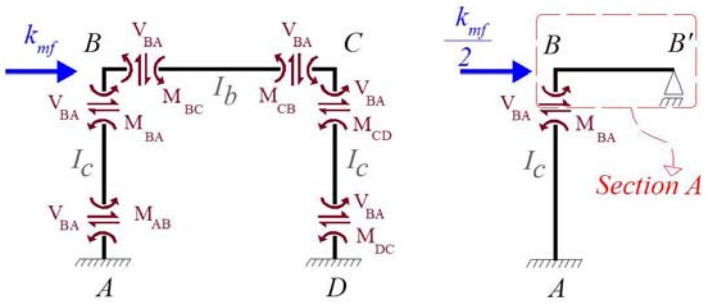

Fig. A1 Distribution of internal forces and moments in moment frame

Eq. (12) was derived by using conventional slope-deflection method. Details are presented as bellow

$$M_{BA}=\frac{2EI_c}{L_c}\left(2\theta_B+\theta_A-\frac{3\Delta}{L_c}\right);\ \ \Delta=1,\ \ \theta_A=0\ \rightarrow\ M_{BA}=\frac{2EI_c}{L_c}\left(2\theta_B-\frac{3}{L_c}\right) \tag{A1}$$

$$M_{BC}=\frac{3EI_c}{(L_b/2)}\left(\theta_B-\frac{\Delta}{(L_b/2)}\right);\ \ \Delta=0\ \rightarrow\ M_{BB}=\frac{3EI_b}{(L_b/2)}\left(\theta_B\right) \tag{A2}$$

Considering equilibrium equation of bending moments in node "*B*" and substituting from Eqs. (A1) and (A2), then θ_B is obtained

$$M_{BC}+M_{BA}=0 \;\rightarrow\; \frac{3EI_b}{(L_b/2)}(\theta_B)+\frac{2EI_C}{L_C}\left(2\theta_B-\frac{3}{L_C}\right)=0$$
$$\rightarrow\; \theta_B\left(\frac{6EI_b}{L_b}+\frac{4EI_C}{L_C}\right)=\frac{6EI_C}{{L_C}^2} \;\rightarrow\; \theta_B=\frac{\frac{6EI_C}{{L_C}^2}}{(\frac{6EI_b}{L_b}+\frac{4EI_C}{L_C})} \tag{A3}$$

Substituting Eq. (A3) in equilibrium of horizontal force for section A, k_{mf} is obtained

$$k_{mf}/2+V_{BA}=0$$
$$\rightarrow\; k_{mf}=-2\frac{\frac{2EI_C}{L_C}\left(\theta_B-\frac{3}{L_C}\right)+\frac{2EI_C}{L_C}\left(2\theta_B-\frac{3}{L_C}\right)}{L_C}=\frac{12EI_C}{{L_C}^3}\left(2\frac{\left(\frac{3EI_C}{L_C}\right)}{\left(\frac{3EI_b}{L_b}+\frac{2EI_C}{L_C}\right)}\right) \tag{A4}$$
$$\rightarrow\; k_{mf}=\frac{12EI_C}{{L_C}^3}\left(\frac{I_C/L_C+6I_b/L_b}{2I_C/L_C+3I_b/L_b}\right)$$

Derivations of elastic stiffness of knee brace frame; k_{ebf}; (Eq. (11))

Considering k_{ebf} as lateral force corresponding to a lateral displacement of one (Fig. 2). In this way, the diagonal member force, F_d, and deflection, Δ_d, is calculated as

$$F_d=\frac{k_{ebf}}{\cos(\phi)} \tag{A5}$$

$$\Delta_d=\frac{F_dL_d}{EA_d} \tag{A6}$$

Suppose knee member is encountered between fully rigid and fully released (hinged) on both ends. Deflection in knee member due to F_d is obtained by average of two aforementioned conditions

$$\Delta_k=\frac{\frac{F_dL_{dke}^3L_{uke}^3}{3EI_kL_k^3}+\frac{F_dL_{dke}^2L_{uke}^2}{3EI_kL_k}}{2} \tag{A7}$$

Relation between unit lateral displacement and diagonal displacement is

$$1 \times \cos(\phi) = \Delta_d + \Delta_k \tag{A8}$$

Substituting Eqs. (A5) to (A7) in Eq. (A8)

$$\cos(\phi) = \frac{k_{ebf} L_d}{\cos(\phi) E A_d} + \frac{k_{ebf}}{\cos(\phi)} \left[\frac{\frac{L_{dke}^3 L_{uke}^3}{3EI_k L_k^3} + \frac{L_{dke}^2 L_{uke}^2}{3EI_k L_k}}{2} \right] \rightarrow \quad k_{ebf} = \frac{\cos^2(\phi)}{\frac{\frac{L_{dke}^3 L_{uke}^3}{3EI_k L_k^3} + \frac{L_{dke}^2 L_{uke}^2}{3EI_k L_k}}{2} + \frac{L_d}{EA_d}} \tag{A9}$$